Laser-induced versus shock wave induced transformation of highly ordered pyrolytic graphite

Citation: Veysset, D.; Pezeril, T.; Kooi, S.; Bulou, A. and Nelson, Keith A. "Laser-Induced Versus Shock Wave Induced Transformation of Highly Ordered Pyrolytic Graphite." Applied Physics Letters 106, no. 16 (April 2015): 161902 © 2015 AIP Publishing LLC

As Published: http://dx.doi.org/10.1063/1.4918929

Publisher: American Institute of Physics (AIP)

Persistent URL: http://hdl.handle.net/1721.1/109265

Version: Author's final manuscript: final author's manuscript post peer review, without publisher's formatting or copy editing

Shock-wave induced formation of nano-crystalline graphite from highly ordered pyrolytic graphite

David Veysset[1,2], Thomas Pezeril[3], Steve Kooi[2], Alain Bulou[3], and Keith Nelson[1,2].

[1]*Department of Chemistry, Massachusetts Institute of Technology, Cambridge, Massachusetts 02139, USA*

[2]*Institute for Solider Nanotechnologies, Massachusetts Institute of Technology, Cambridge, Massachusetts 02139, USA*

[3]*Institut Molécules et Matériaux du Mans, UMR CNRS 6283, Université du Maine, 72085 Le Mans, France*

Abstract

We demonstrate that in-plane 2D propagation and focusing of a laser-induced shock wave results in enhanced nano-crystallization of highly ordered pyrolytic graphite. Throughout the 2D shock focusing technique, which enables to clearly distinguish between the laser-induced and the shock-induced transformation/transition, our findings establish the role of the shock wave during the transformation/transition process. This novel configuration could open the way to an alternative path for laser shock fabrication of graphitic compounds and would give access to real time investigation of shock waves mediated phase transitions.

Many carbon allotropes, natural and man-made, are widely studied for their fundamental interest and their useful physical and chemical properties. A standard is set by diamond with its extremely strong sp3 covalent bonding and with the highest hardness and thermal conductivity of any bulk material. Different forms of carbon allotropes including diamond-like carbons (DLC) and graphitic carbons [1,2] are used in applications such as protective coatings and batteries. Today, most commercially available nano-diamonds are prepared by detonation methods [3], chemical vapor deposition [4], laser irradiation of graphite [5–7], or carbon black [8], but often with low yield or requiring post-formation

purification treatments. New routes of synthesis would stem from a better understanding of the transitions between different phases or local structures. The formation of diamond-like carbon and nano-diamond from highly ordered pyrolytic graphite (HOPG) has been investigated by many groups. Depending on the crystalline grade and orientational order of the starting material, a wide range of transition onset pressures have been observed. Erskine and Nellis carried out shock experiments on HOPG up to 50 GPa with the shock normal to the basal plane and observed a martensitic transformation of HOPG to diamond-like carbon at 19.6 GPa [9]. Yamada and Tanabe reported the phase transition to diamond and diamond-like carbon at pressures of 15 GPa with a shock propagating along the basal plane [10]. More recently, Nian et al. synthesized nano-diamonds from graphite through direct low intensity laser irradiation using a transparent confinement layer to generate a local high dense plasma. The pressure was estimated to be 4.4 GPa [11].

Here we report formation of a nano-crystalline graphitic phase from HOPG through in-plane 2D focusing of a laser-induced shock wave. The approach we present allows spatial separation of the sample regions into which the laser light and the focused shock wave are directed, permitting direct visualization of the shocked region and confirmation that the shock wave drives the material transformation. The laser light also generates nano-crystalline graphitic carbon, but in a distinct sample region. Our results provide a new experimental pathway for nano-crystalline graphite formation driven by laser-generated shock waves.

Experimental

The sample consists of 5 µm thick highly oriented pyrolytic graphite (HOPG) (SPI Supplies ®), sandwiched between two 1-inch diameter silica glass plates, 100 µm and 300 µm thick, that hold the sample vertically (see Fig. 1(a)). The 5 µm thick HOPG samples are obtained by pulling off layers from the HOPG substrate using a piece of tape (3M© Scotch Brand, 62 µm thick).The freshly cleaved surface is in contact with the 100 µm substrate. The tape is not removed and remains in contact with the 300 µm substrate.

A laser excitation pulse of 300 ps duration and 800 nm wavelength, derived from the uncompressed output of a Ti:sapphire amplifier, is directed onto an axicon conical prism and focused by a lens to form a 200 µm diameter ring pattern at the sample surface, generating a focusing shock wave as described previously [12] (see Fig 1(a)). The beam at any part of the ring has a width of 10 µm. The shock waves are generated at the surface of the graphite substrate through strong absorption of the excitation pulse. Two counter-propagating shock waves are launched laterally in the plane of the sample, along the basal plane of the HOPG. As a consequence of the laser excitation ring pattern, one of the shock waves propagates and focuses inward toward the center while the second propagates outward and diverges (see Fig. 1(b)). Each shot damages the HOPG surface either through direct irradiation (in the region of the excitation ring pattern) or through the resulting shock waves across an area of several hundred microns diameter. After each shot, the sample, mounted on a motorized stage, is translated to an undisturbed area. Once the HOPG sample is ready for analysis of the shocked areas, the 100 µm glass substrate is removed, and the sample is examined using a Raman spectrometer.

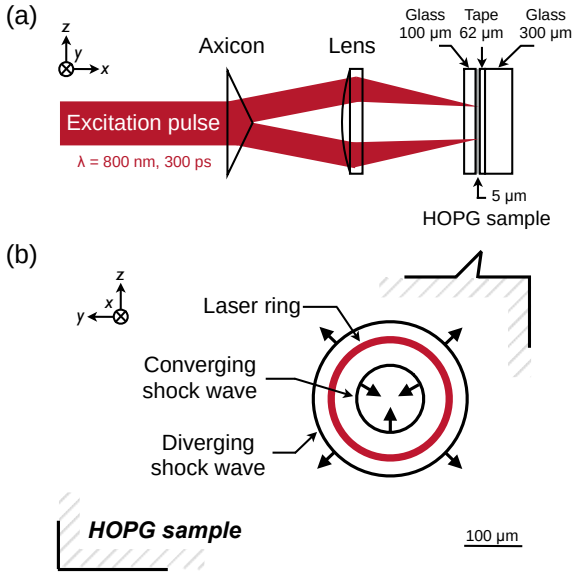

FIG. 1. (Color online) (a) The laser excitation pulse is focused by an axicon-lens combination into a ring pattern at the sandwiched HOPG sample. (b) Converging and diverging shock waves (black circles) emanate from the irradiated area (red circle) at the HOPG surface. The laser excitation ring has a diameter of 200 µm and a width of 10 µm.

Raman spectroscopy is the most common method of investigation for carbon materials [13]. It allows fast and non-destructive analysis with micron spatial resolution. Raman spectra were acquired at different locations on the sample surface using a Raman microscope system equipped with an imaging CCD and a motorized stage allowing for simple identification of the laser-irradiated and shocked regions. The Raman excitation laser wavelength was 632.8 nm, and Raman spectra were obtained in a backscattering configuration using a 100 × objective (NA 0.90). The system provided overall spatial resolution of 4 μm. The Raman probing depth is limited by the penetration depth excitation of the laser light to about 70 nm.

The main features present in the Raman spectra of graphitic materials were first described by Tuinstra & Koenig [14]. The spectrum of the starting material (Fig. 2, bottom spectrum) is typical of high purity commercial graphite with a strong G band at 1585 cm^{-1}. The second-order phonon 2D bands at about 2700 cm^{-1} consist of two components 2D(1) and 2D(2) characteristic of bulk graphite [15].The Raman spectrum of the shocked material for a laser excitation fluence of 24.0 J/cm^2, recorded at the shock focus where the shock pressure is expected to have been at its maximum, is shown in Fig. 2 (top spectrum and inset). The spectrum is typical of disordered graphite [16,17], with substantial broadening of the G band and another strong band, conventionally labeled D, appearing at lower frequency. The different peaks have been studied extensively and assigned as follows. The G band at 1585 cm^{-1} arises from stretching modes of all pairs of sp^2 atoms in chains and rings (E_{2g} mode). The D (or D_1) band and a weaker band labeled D' (or D_2), usually found respectively at about 1350 cm^{-1}, and 1620 cm^{-1} (the latter a weak shoulder of the G band), are disorder-induced. D_3 and D_4 are respectively attributed to amorphous carbon and disordered graphitic lattice [18]. The D band in the shocked material spectrum and the 2D bands in the HOPG spectrum originate from a double resonant Raman scattering process as shown by Thomsen and Reich [19]. A D-G combination band appears in the shocked material spectrum at 2950 cm^{-1}, also induced by the increase of disorder [20]. The D and D' modes only become active in the presence of disorder and therefore do not appear in perfect graphite. In addition, the doublet

structure of the 2D band, present in bulk graphite and indicative of c-axis ordering, is lost in the shocked sample [20]. As explained by Ferrari [15], (i) the increase in the I_D/I_G ratio, (ii) the appearance of the D' peak, (iii) the loss of the doublet structure of the 2D mode, and (iv) the broadening of the peaks are all clear indications of the transformation from graphite to nano-graphite, which is the first stage in the amorphization trajectory [13,21]. The intensity ratio between the D band and G band peaks (I_D/I_G) is often taken as the first criterion for disorder evaluation in graphitic materials [14,17]. We fit the spectra from many sample regions using the five contributions indicated in previous work [18] and described above, and compared the ratio determined from the fits to the ratio extracted directly from the two strong peak heights in the spectra. The values typically agreed to within 15%, so for purposes of mapping as described below we simply used the observed peak heights.

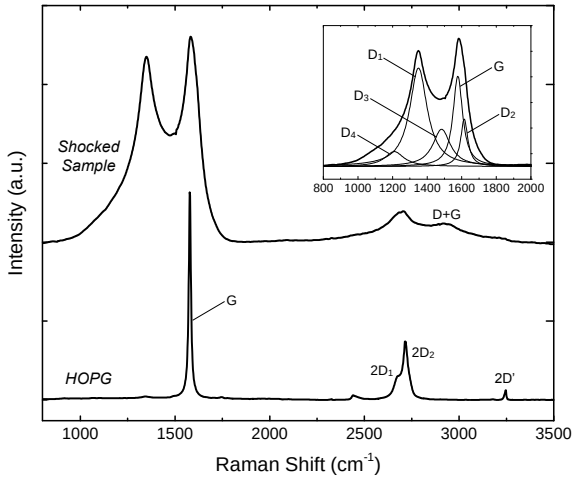

FIG. 2. Raman spectra of commercial HOPG (starting material) and shocked sample. The top spectrum was recorded at the center of the excitation ring for a laser excitation pulse fluence of 24.0 J/cm^2. (Inset) The Raman peaks of the shocked samples were fitted using a five-band fitting procedure with four Lorentzian bands (G, D or D_1, D or D_2, and D_4) and one Gaussian band (D_3) to extract their positions, heights and widths following Sadezky et al. [18]. The strongest two peaks that are conventionally labeled D and G, give here a fitted peak height ratio ID/IG of about 1.1.

The laser excitation pulse energy was varied to control the shock pressure at the center of convergence. Scanning electron micrographs of shocked samples are shown Fig. 3(a) and Fig. 3(b) for two different laser excitation fluences, 8.0 and 24.0 J/cm^2. Areas that were exposed to the laser light are easily located under both optical and scanning electron microscopes. Those areas as well as regions near them and around the center where the shock was focused clearly show permanent sample damage. For low laser fluence (8.0 J/cm^2), optical observation of the back faces of the graphite samples did not show significant damage. However, for higher laser fluence (24.0 J/cm^2), the graphite layer is damaged over its entire thickness due to the higher pressure generated upon laser absorption. Raman spectra were collected over a 400 μm by 400 μm square region covering the entire shocked areas, with the laser light probing a 4 μm diameter spot and with 4 μm steps between successive measurements. Fig. 3(c) and Fig. 3(d) present maps of the I_D/I_G ratio from the same samples shown respectively in Fig. 3(a) and Fig. 3(b). As shown in Fig. 3(c), the substantially higher I_D/I_G ratio at the ring location compared to the initial HOPG I_D/I_G ratio reveals the highly disordered phase, i.e. nano-crystalline graphite phase, caused by direct laser irradiation. The I_D/I_G ratio decreases away from the excitation ring, then increases around the center to reach its maximum (of about 1.0) at the shock focal point attesting to the shock-induced nano-crystallization. For a higher laser excitation fluence of 24.0 J/cm^2 (Fig. 3(d)), an area of about 300 μm in diameter shows an increase in the I_D/I_G ratio. Again, a greater degree of nano-crystallization is indicated at the shock wave focal point than at the laser irradiation region. Figure 4 shows a high magnification SEM image recorded from the shock focal region of the sample shown in Figs. 3(b) and 3(d). At the center of the shock focus, the HOPG shows a dramatic change in its structure. The sample consists of graphitic nano-crystalline structures with a characteristic size scale of about 100 nm. Thus the disorder to which the Raman spectral features in the shocked samples are attributed is clearly present. A high magnification image of an unshocked sample (upper left corner of Fig. 4) shows no such disorder.

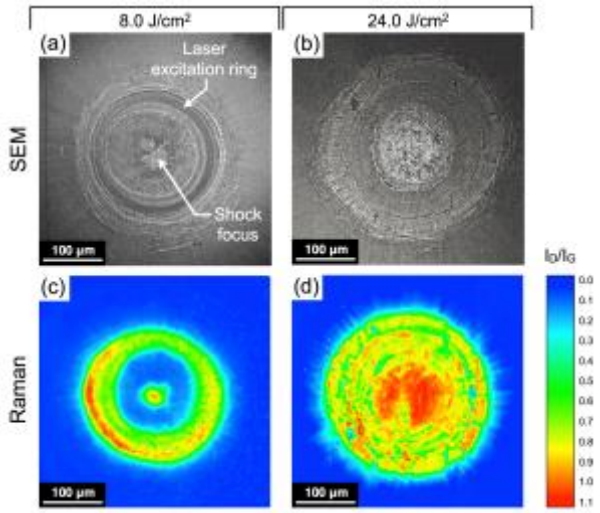

FIG. 1. (Color online) SEM images of shocked samples for laser excitation fluences of (a) 8.0 J/cm^2 and (b) 24.0 J/cm^2. (a) The laser irradiated ring area appears in dark grey. A shock wave was focused toward the center of the ring, leaving permanent structural change in the graphite at the center that appears in the image as a lighter grey. (b) For higher laser excitation fluence, the entire damaged area is larger, extending to a radius of 150 μm. (c),(d) I_D/I_G ratio mapping of the surfaces of the shocked samples shown in (a) and (b) respectively. (c) The ratio is significantly increased at the excitation ring and at the shock focus, indicating nano-crystallization of the graphite under both laser irradiation and shock loading. At the center of the shock focus, the ratio reaches about 1.0. (d) For higher excitation fluence, the nano-crystallization covers a larger area, including the entire region inside the excitation ring and some material outside where the diverging shock wave propagated. The highest ratio appears around the shock focal region.

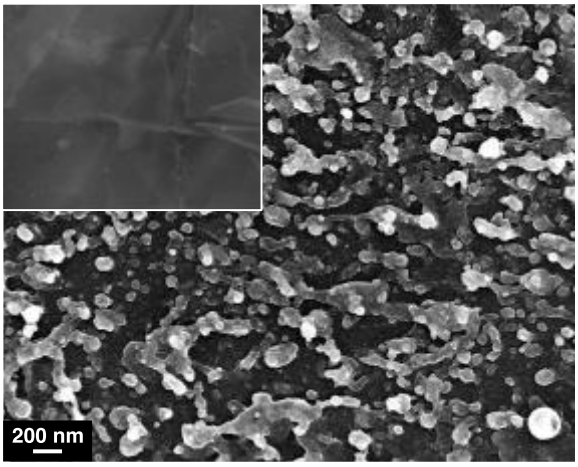

FIG. 4**.** High magnification SEM micrograph taken at the center of the shock focus for the sample shown in Figs. 3(b) and 3(d) revealing the nano-structure of the shocked HOPG. (Inset) SEM micrograph of the starting HOPG material.

Discussion

In our configuration where the HOPG is confined behind a transparent window, it is possible to estimate the pressure rise in the material upon laser absorption and plasma generation according to the model developed by Fabbro et al. [22]. Considering the shock impedances of the glass substrate and the HOPG, our calculations show that for a laser fluence of 24 J/cm^2 (or laser intensity of 80 GW/cm^2) the pressure at the laser-irradiated ring location reaches about 15 GPa. For that laser fluence, the I_D/I_G ratio is greater at the shock focus than at the laser excitation ring, suggesting comparable or higher pressure at the shock focus. The comparison between regions is only qualitative since both regions are also heated substantially. Based on the work of Ren et al. [23] we estimate the temperature in the laser-irradiated carbon plasma to be above 4000 K, and the temperature at the shock focus may be comparable [12]. We estimate the laser-induced shock duration to have an upper limit of about 450 ps which is the acoustic propagation time across the width of the shock wave (given by the 10 μm excitation laser line width). The shock speed exceeds the acoustic speed so the shock duration was shorter. We do not have information about the depth of the transformed region, but we expect the shock response to extend deeper into the sample than our Raman probe can see which is 70 nm.

No clear evidence of diamond or nano-diamond formation was found from Raman or fluorescence spectra, x-ray diffraction measurements, or TEM imaging. Several possible reasons could explain the failure to detect diamond. First, the quantity of diamond, or most likely nano-diamond, formed might be too small to be detected. The x-ray diffraction measurements were conducted with intrinsically coarse in-plane and in-depth resolution, without high sensitivity to the center of shock convergence where the shock pressure and the associated high temperature were greatest. The Raman scattering efficiency of graphite is about 50 times higher than that of diamond for visible Raman excitation wavelengths [24]. Techniques to chemically isolate nano-diamonds [23] might allow their detection. However, according to a suggested weak spots mechanism for diamond formation [25,26], the transition from graphite to diamond occurs through a diffusional reconstructive process where both pressure and temperature play major roles. Recent investigations of the growth mechanism of nano-crystalline diamond via laser processing highlighted the importance of shock wave dynamics at nanosecond time scales [25]. Indeed, sustained high temperature and high pressure conditions promote diamond nucleation, and the rate of temperature and pressure drop accompanying the rarefaction wave determines the extent of regraphitization of the diamond crystallites [10]. The shock duration of several hundred picoseconds in our experiments may be too short to promote sufficient diamond growth and retention. Different excitation conditions that generate longer duration shocks may be more favorable for nano-diamond formation.

Conclusions

We have presented a novel configuration that opens alternative prospects for controlled transformations from graphitic starting materials. We have demonstrated structural transformation of graphite into nano-crystalline graphite induced by focusing shock waves at the micro-scale. As an extension, based on our earlier time-resolved observations of focusing shock waves in liquids, we envision time-resolved visualization and spectroscopic measurement of phase transitions as they are under way. Other shock-mediated phase transitions such as ferroelectric, magnetic, and electronic phase

transitions could be investigated with unique capabilities for temporally and spatially resolved observation and for samples [27,28] that are unavailable in large quantities or sizes that might be needed for conventional shock experiments.

Acknowledgment

This material is based upon work supported in part by the U. S. Army Research Laboratory and the U.S. Army Research Office through the Institute for Soldier Nanotechnologies, under contract number W911NF-13-D-0001. The authors gratefully acknowledge Rudolf Bratschitsch for the photoluminescence experiments, Marie-Pierre Crosnier-Lopez for TEM images, Guillaume Brotons for SAXS experiments, Alex Maznev, Alexey Lomonosov, and Pavel Zinin for fruitful discussions.

Bibliography

[1] Grill A. Diamond-like carbon coatings as biocompatible materials—an overview. Diam Relat Mater 2003;12:166–70. doi:10.1016/S0925-9635(03)00018-9.

[2] Endo M, Hayashi T, Kim YA, Muramatsu H. Development and Application of Carbon Nanotubes. Jpn J Appl Phys 2006;45:4883–92. doi:10.1143/JJAP.45.4883.

[3] Danilenko V V. On the history of the discovery of nanodiamond synthesis. Phys Solid State 2004;46:595–9. doi:10.1134/1.1711431.

[4] Sharda T, Rahaman MM, Nukaya Y, Soga T, Jimbo T, Umeno M. Structural and optical properties of diamond and nano-diamond films grown by microwave plasma chemical vapor deposition. Diam Relat Mater 2001;10:561–7. doi:10.1016/S0925-9635(00)00390-3.

[5] Ogale S, Malshe A, Kanetkar S., Kshirsagar S. Formation of diamond particulates by pulsed ruby laser irradiation of graphite immersed in benzene. Solid State Commun 1992;84:371–3. doi:10.1016/0038-1098(92)90479-S.

[6] Yang G-W, Wang J-B, Liu Q-X. Preparation of nano-crystalline diamonds using pulsed laser induced reactive quenching. J Phys Condens Matter 1998;10:7923–7. doi:10.1088/0953-8984/10/35/024.

[7] Nüske R, Jurgilaitis A, Enquist H, Harb M, Fang Y, Håkanson U, et al. Transforming graphite to nanoscale diamonds by a femtosecond laser pulse. Appl Phys Lett 2012;100:043102. doi:10.1063/1.3678190.

[8] Hu S, Tian F, Bai P, Cao S, Sun J, Yang J. Synthesis and luminescence of nanodiamonds from carbon black. Mater Sci 2009;157:11–4. doi:10.1016/j.mseb.2008.12.001.

[9] Erskine DJ, Nellis WJ. Shock-induced martensitic transformation of highly oriented graphite to diamond. J Appl Phys 1992;71:4882. doi:10.1063/1.350633.

[10] Yamada K, Tanabe Y. Shock-induced phase transition of oriented pyrolytic graphite to diamond at pressures up to 15 GPa. Carbon N Y 2002;40:261–9. doi:10.1016/S0008-6223(01)00086-0.

[11] Nian Q, Wang Y, Yang Y, Li J, Zhang MY, Shao J, et al. Direct Laser Writing of Nanodiamond Films from Graphite under Ambient Conditions. Sci Rep 2014;4:6612. doi:10.1038/srep06612.

[12] Pezeril T, Saini G, Veysset D, Kooi S, Fidkowski P, Radovitzky R, et al. Direct visualization of laser-driven focusing shock waves. Phys Rev Lett 2011;106:1–4. doi:10.1103/PhysRevLett.106.214503.

[13] Ferrari AC, Robertson J. Raman spectroscopy of amorphous, nanostructured, diamond-like carbon, and nanodiamond. Philos Trans A Math Phys Eng Sci 2004;362:2477–512. doi:10.1098/rsta.2004.1452.

[14] Tuinstra F, Koenig JL. Raman spectrum of graphite. J Chem Phys 1970;53:1126–30.

[15] Ferrari AC. Raman spectroscopy of graphene and graphite: Disorder, electron-phonon coupling, doping and nonadiabatic effects. Solid State Commun 2007;143:47–57. doi:10.1016/j.ssc.2007.03.052.

[16] Lespade P, Al-Jishi R, Dresselhaus MS. Model for Raman scattering from incompletely graphitized carbons. Carbon N Y 1982;20:427–31. doi:10.1016/0008-6223(82)90043-4.

[17] Wopenka B, Pasteris JD. Strucfural characterizxtion of kerogens to granulite-facies gaphite : Applicability of Raman microprobe spectroscopy. Am Mineral 1993;78:533–57.

[18] Sadezky A, Muckenhuber H, Grothe H, Niessner R, Pöschl U. Raman microspectroscopy of soot and related carbonaceous materials: Spectral analysis and structural information. Carbon N Y 2005;43:1731–42. doi:10.1016/j.carbon.2005.02.018.

[19] Thomsen C, Reich S. Double Resonant Raman Scattering in Graphite. Phys Rev Lett 2000;85:5214–7. doi:http://dx.doi.org/10.1103/PhysRevLett.85.5214.

[20] Pimenta MA, Dresselhaus G, Dresselhaus MS, Cançado LG, Jorio A, Saito R. Studying disorder in graphite-based systems by Raman spectroscopy. Phys Chem Chem Phys 2007;9:1276–91. doi:10.1039/b613962k.

[21] Lespade P, Marchand A, Couzi M, Cruege F. Caracterisation de materiaux carbones par microspectrometrie Raman. Carbon N Y 1984;22:375–85. doi:10.1016/0008-6223(84)90009-5.

[22] Fabbro R, Fournier J, Ballard P, Devaux D, Virmont J. Physical study of laser-produced plasma in confined geometry. J Appl Phys 1990;68:775–84. doi:10.1063/1.346783.

[23] Ren XD, Yang HM, Zheng LM, Yuan SQ, Tang SX, Ren NF, et al. A conversion model of graphite to ultrananocrystalline diamond via laser processing at ambient

temperature and normal pressure. Appl Phys Lett 2014;105:16–20. doi:10.1063/1.4890527.

[24] Wagner J, Ramsteiner M, Wild C, Koidl P. Resonant Raman scattering of amorphous carbon and polycrystalline diamond films. Phys Rev B 1989;40:1817–24. doi:10.1103/PhysRevB.40.1817.

[25] Morris DG. An investigation of the shock-induced transformation of graphite to diamond. J Appl Phys 1980;51:2059–65. doi:10.1063/1.327873.

[26] Kleiman J, Heimann RB, Hawken D, Salansky NM. Shock compression and flash heating of graphite/metal mixtures at temperatures up to 3200 K and pressures up to 25 GPa. J Appl Phys 1984;56:1440. doi:10.1063/1.334116.

[27] Collet E, Lemée-Cailleau M-H, Buron-Le Cointe M, Cailleau H, Wulff M, Luty T, et al. Laser-induced ferroelectric structural order in an organic charge-transfer crystal. Science 2003;300:612–5. doi:10.1126/science.1082001.

[28] Cammarata M, Bertoni R, Lorenc M, Cailleau H, Di Matteo S, Mauriac C, et al. Sequential Activation of Molecular Breathing and Bending during Spin-Crossover Photoswitching Revealed by Femtosecond Optical and X-Ray Absorption Spectroscopy. Phys Rev Lett 2014;113:227402. doi:http://dx.doi.org/10.1103/PhysRevLett.113.227402.